Particulate Matter Disrupts Human Lung Endothelial Barrier Integrity via ROS- and p38 MAPK–Dependent Pathways

Ting Wang[1], Eddie T. Chiang[1], Liliana Moreno-Vinasco[1], Gabriel D. Lang[1], Srikanth Pendyala[1], Jonathan M. Samet[2], Alison S. Geyh[3], Patrick N. Breysse[3], Steven N. Chillrud[4], Viswanathan Natarajan[1], and Joe G. N. Garcia[1]

[1]Department of Medicine, Section of Pulmonary and Critical Care Medicine, University of Chicago, Chicago, Illinois; Departments of [2]Epidemiology and [3]Environmental Health Sciences, Bloomberg School of Public Health, Johns Hopkins University, Baltimore, Maryland; and [4]Lamont Doherty Earth Observatory, Columbia University, Palisades, New York

Epidemiologic studies have linked exposure to airborne pollutant particulate matter (PM) with increased cardiopulmonary mortality and morbidity. The mechanisms of PM-mediated lung pathophysiology, however, remain unknown. We tested the hypothesis that PM, via enhanced oxidative stress, disrupts lung endothelial cell (EC) barrier integrity, thereby enhancing organ dysfunction. Using PM collected from Ft. McHenry Tunnel (Baltimore, MD), we assessed PM-mediated changes in transendothelial electrical resistance (TER) (a highly sensitive measure of barrier function), reactive oxygen species (ROS) generation, and p38 mitogen-activated protein kinase (MAPK) activation in human pulmonary artery EC. PM induced significant dose (10–100 μg/ml)- and time (0–10 h)-dependent EC barrier disruption reflected by reduced TER values. Exposure of human lung EC to PM resulted in significant ROS generation, which was directly involved in PM-mediated EC barrier dysfunction, as N-acetyl-cysteine (NAC, 5 mM) pretreatment abolished both ROS production and barrier disruption induced by PM. Furthermore, PM induced p38 MAPK activation and HSP27 phosphorylation, events that were both attenuated by NAC. In addition, PM-induced EC barrier disruption was partially prevented by the p38 MAP kinase inhibitor SB203580 (10 μM) as well as by reduced expression of either p38 MAPK β or HSP27 (siRNA). These results demonstrate that PM induces ROS generation in human lung endothelium, resulting in oxidative stress–mediated EC barrier disruption via p38 MAPK- and HSP27-dependent pathways. These findings support a novel mechanism for PM-induced lung dysfunction and adverse cardiopulmonary outcomes.

Keywords: endothelial permeability; HSP27; particulate matter; p38 MAP kinase; ROS

CLINICAL RELEVANCE

This study demonstrates that particulate matter (PM) induces reactive oxygen species generation in human lung endothelium, resulting in oxidative stress–mediated endothelial cell barrier disruption via p38 mitogen-activated protein kinase– and HSP27-dependent pathways. These findings support a novel mechanism for PM-induced lung dysfunction and potential adverse cardiovascular outcomes.

Growing epidemiologic evidence supports the linkage of exposure to ambient particulate matter (PM) to deleterious cardiopulmonary health effects and increased cardiopulmonary mortality and morbidity (1). Exposure risk is especially increased in susceptible populations including individuals with asthma, chronic obstructive pulmonary disease (COPD), cardiac arrhythmias, and congestive heart failure (CHF). Various mechanisms have been proposed to explain the cardiopulmonary health effects of PM, including pulmonary and systemic oxidative stress and inflammation (2), enhanced coagulation (3), and altered cardiac autonomic function (4).

After inhalation, fine/ultrafine PM passes rapidly into systemic circulation, potentially interacting with endothelial cells (ECs) (5) with induction of atherosclerotic plaque formation (6), endothelium-dependent dilation in the systemic microcirculation (7), and increased oxidative stress in vascular EC via NAD(P)H oxidase and mitochondrial pathways (8). Although the actual mechanism(s) for PM-mediated acceleration of cardiopulmonary events is unknown, it is likely to be multifaceted, with endothelial dysfunction as a critical component.

We recently described in a murine model strong evidence for PM-mediated vascular barrier dysfunction with increased protein leakage into bronchoalveolar lavage (BAL) (9), a marker of acute inflammatory lung damage (10). Increased endothelial monolayer permeability is also observed in inflammatory pulmonary conditions, such as acute lung injury (ALI), acute respiratory distress syndrome (ARDS), sepsis (11), and devastating lung disorders with mortality exceeding 30% (12), as well as more subacute and chronic inflammatory disorders such as asthma.

We hypothesized that PM may directly disrupt pulmonary EC barrier integrity, thereby contributing to acute inflammatory lung permeability *in vivo*. To test this hypothesis *in vitro*, we cultured human pulmonary artery ECs on gold electrodes and assessed transendothelial electrical resistance (TER) across EC monolayers as a marker of barrier integrity. In addition, we investigated the involvement of reactive oxygen species (ROS) and mitogen-activated protein kinase (MAPK) signaling pathways and now provide evidence that PM produces EC barrier dysfunction through ROS-dependent p38 MAPK activation. These results increase our understanding of PM-induced adverse cardiopulmonary outcomes.

(*Received in original form October 10, 2008 and in final form April 26, 2009*)

These studies were supported by Environmental Protection Agency/Johns Hopkins Particulate Matter Center Grant # RD83241701 (J.G.N.G. and J.M.S.) and National Institutes of Health HL058064-13 (J.G.N.G.).

Disclaimer: Although the research described in this article has been funded in part by the United States Environmental Protection Agency through grant/cooperative agreement # RD-83241701, it has not been subjected to the Agency's required peer and policy review and therefore does not necessarily reflect the views of the Agency, and no official endorsement should be inferred.

Correspondence and requests for reprints should be addressed to Joe G. N. Garcia, M.D., Department of Medicine, University of Chicago Pritzker School of Medicine, 5841 S. Maryland Avenue, W604, Chicago, IL 60637. E-mail: jgarcia@medicine.bsd.uchicago.edu

This article has an online supplement, which is accessible from this issue's table of contents at www.atsjournals.org

Am J Respir Cell Mol Biol Vol 42. pp 442–449, 2010
Originally Published in Press as DOI: 10.1165/rcmb.2008-0402OC on June 11, 2009
Internet address: www.atsjournals.org

MATERIALS AND METHODS

Reagents and Chemicals

Molecular mass standards, polyacrylamide gels, buffers, and protein assay reagents were purchased from Bio-Rad (Hercules, CA). Antibodies were purchased from Cell Signaling (Danvers, MA), and all other chemicals and reagents were obtained from Sigma-Aldrich Co. (St. Louis, MO) unless stated otherwise.

Collection and Characterization of PM

PM was collected (April of 2005) from the Ft. McHenry Tunnel, Baltimore, MD using a high-volume cyclone collector. The cyclone collects particles greater than 0.1–0.3 μm in aerodynamic diameter. Traffic within the tunnel included both truck and passenger vehicles. Samples were collected a flow rate of 1.0 m^3/minute in the lumen of the tunnel over a 1-month period. PM was harvested from the collection cup and the body of the cyclone. The high-volume cyclone collector has been used to collect PM for a variety of *in vivo* and *in vitro* studies (9, 13–18).

Analysis for elemental metals content was conducted by high-resolution ICP-MS (Element Finnegan, Mat Breman, Germany). Sample digestion was conducted in a Milestone MEGA microwave digestion oven (Model Mega MLS 1200; Milestone, Monroe, CT). Nitric acid and hydrofluoric acid used for sample digestion were Optima Grade (Fisher Scientific, Columbia, MD). Samples and procedural blanks from digestion batches were analyzed on the same day. Data were collected for all isotopes of interest at the appropriate resolving power (RP) to avoid isobaric interferences. Indium was added to all samples, blanks, and standards as an internal standard and run in all resolving powers. Quantification was done by external and internal standardization. Data were drift-corrected using indium, quantified, converted to a mass, and corrected for blanks. Samples that were below the LOQ based on daily procedural blanks were flagged. Indium-corrected elemental sensitivities in either matrix routinely differ by less than 5% sample for all elements. Elemental composition (micrograms per gram) representing the most abundant constituents included aluminum (17,533.74), copper (8,777.886), iron (132,545.9), lead (240.8274), calcium (47,263.08), sodium (8,068.263), potassium (5,102.741), magnesium (7,332.056), titanium (3,197.332), and zinc (8,777.886). PM was stored at ambient temperature in the dark.

Cell Culture

Human pulmonary artery ECs obtained from Lonza (Basel, Switzerland) were cultured as previously described (19) in EGM-2 complete medium (Lonza) with 10% fetal bovine serum at 37°C in a humidified atmosphere of 5% CO2/95% air, with passages 6 to 10 used for experimentation. Before PM challenge (24 h), EC media was changed to EGM-2 with 2% fetal bovine serum (Lonza).

Transendothelial Electrical Resistance

Endothelial cells were grown to confluence in polycarbonate wells containing evaporated gold microelectrodes, and TER measurements obtained using an electrical cell-substrate impedance sensing system (ECIS) (Applied Biophysics, Troy, NY) as previously described in detail (20, 21). TER values from each microelectrode were pooled at discrete time points and plotted versus time as the mean ± SE (21). The effect of PM was calculated as Δ (TER_{PM} − $TER_{control}$), or $\Delta(TER_{inhibitor\ +\ PM} - TER_{inhibitor\ only})$ when an inhibitor or siRNA was used. The confluent EC on the electrode achieves a TER value around 1,400 to 1,700 ohm.

ROS Detection by Fluorescence Microscopy

Formation of ROS in ECs was quantified by fluorescence microscopy (22). Human lung ECs (~ 90% confluent) in 35-mm dishes were loaded with DCFDA (10 μM) in EBM-2 basal medium for 30 minutes at 37°C in a 95% air, 5% CO_2 environment. After 30 minutes of incubation, the medium containing DCFDA was aspirated, and the cells were rinsed once with EGM-2 complete medium and then pre-incubated with agents for the indicated time periods. At the end of the incubation, the cells were washed twice with phosphate-buffered saline (PBS) at room temperature and examined under a Nikon (Melville, NY) Eclipse TE 300 microscope and Sony (New York, NY) Digital Photo camera DKC 5000 with all images recorded and stored.

Transfection and Infection of Endothelial Cells

The siRNA sequence(s) targeting α, β, γ, and delta isoforms of human p38 MAPK and human HSP27 were purchased from Dharmacon RNA Technologies, Inc. (Lafayette, CO). Human lung ECs were then transfected with siRNA using siPORT Amine (Ambion, Austin, TX) as the transfection reagent according to the manufacturer's protocol. Cells (~40% confluent) were serum-starved for 1 hour, followed by incubation with 100 ng/ml total target siRNA (or control siRNA) for 6 hours in serum-free medium. Serum-containing medium was then added (10% serum final concentration) for 42 hours before biochemical experiments and/or functional assays were conducted.

Western Blot

EC cell lysate was prepared after indicated treatment as previously described (18). Equal amounts of protein samples were separated on SDS/PAGE, transferred to nitrocellular membranes, blocked with 5% BSA in TBS-Tween20 (0.5%) for 1 hour, and incubated with primary antibodies in 5% (wt/vol) BSA in TBS-Tween20 overnight at 4°C. The primary antibody was detected by incubation with horseradish peroxidase–coupled second antibody (1:2,000 in TBS-Tween20 with 5% BSA) at room temperature for 2 hours. The chemiluminescence detection was performed by using Chemiluminescence Reagent from Cell Signaling (Danvers, MA).

Endothelial Cell Imaging

ECs were grown on gelatinized coverslips before exposure to various conditions as described for individual experiments. EC were then fixed in 3.7% formaldehyde and permeabilized with 0.25% Triton X-100 for 5 minutes. Cells were washed in PBS, blocked with 2% bovine serum albumin in PBS for 30 minutes, and then incubated for 60 minutes at room temperature with Texas Red–conjugated phalloidin for F-actin

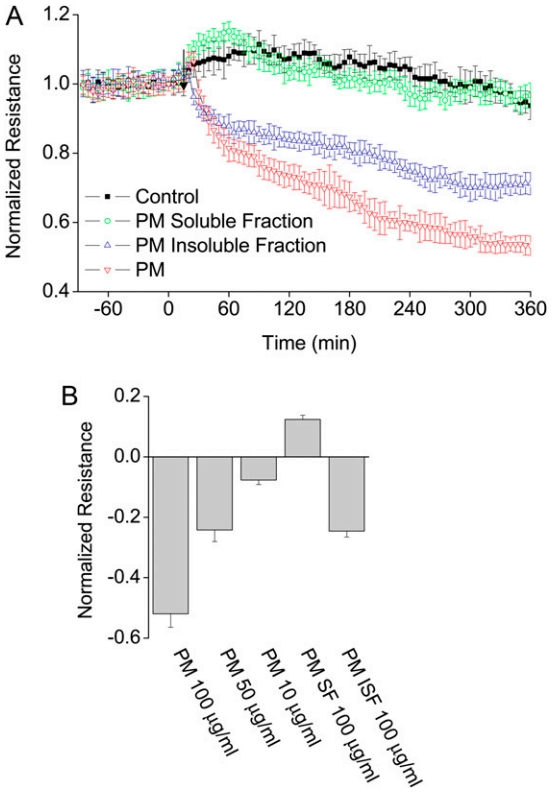

Figure 1. Baltimore tunnel particulate matter (PM) induces human lung endothelial cell barrier disruption. (*A*) Both the intact PM preparation and PM insoluble fraction (PM-ISF), but not PM soluble fraction (PM-SF), produced a time-dependent (0–6 h) decline in electrical resistance, indicative of endothelial cell (EC) barrier disruption. (*B*) Bar graph summarized from three independent experiments represents PM-induced dose-dependent (10–100 μg/ml) EC barrier disruption.

staining for 60 minutes at room temperature. After further washing with PBS, coverslips were mounted using Slow Fade (Molecular Probes, Inc., Eugene, OR) and analyzed using a Nikon Eclipse TE 300 microscope and Sony Digital Photo camera DKC 5000. Confocal microscopy was performed using the Radiance Laser scanning 2100 system (Bio-Rad). Images were recorded and stored.

Statistical Analysis

Data are presented as group means ± SE. We performed statistical comparisons by an unpaired Student's *t* test for two groups. In all cases, we defined statistical significance as $P < 0.05$.

RESULTS

PM Disrupts Endothelial Cell Barrier Function

Our initial experiments assessed the effect of PM and water soluble/insoluble PM fractions on human pulmonary EC barrier function as measured by TER, a highly sensitive measure of permeability. PM produced a sustained dose-dependent decrease in TER (indicative of enhanced EC barrier dysfunction) over a range of 10 to 100 μg/ml, with a maximal effect observed at 100 μg/ml (50% decrease in TER). The TER value achieved a steady state approximately 6 hours after PM treatment (Figure 1A). In contrast, the water-soluble PM fraction (supernatant of 100 μg/ml of the intact PM preparation, PM-SF) caused a transient 10% increase in TER, which returned to a baseline value after 30 to 60 minutes. The water-insoluble PM fraction (PM-ISF, 100 μg/ml of the intact PM preparation) induced an effect similar to that of the whole PM preparation. The TER reached a steady state after 5 to 6 hours of PM-ISF treatment (25% decrease in TER). PM did not induce significant EC cell death within 24 hours of treatment (*see* Figure E1 in the online supplement), which strongly suggests that PM mediates significant cytoskeleton rearrangement resulting in EC barrier disruption.

PM-Induced ROS Generation Contributes to Endothelial Cell Barrier Disruption

Strong evidence supports PM as a stimulus for increased endothelial oxidative stress via NADPH oxidase activation

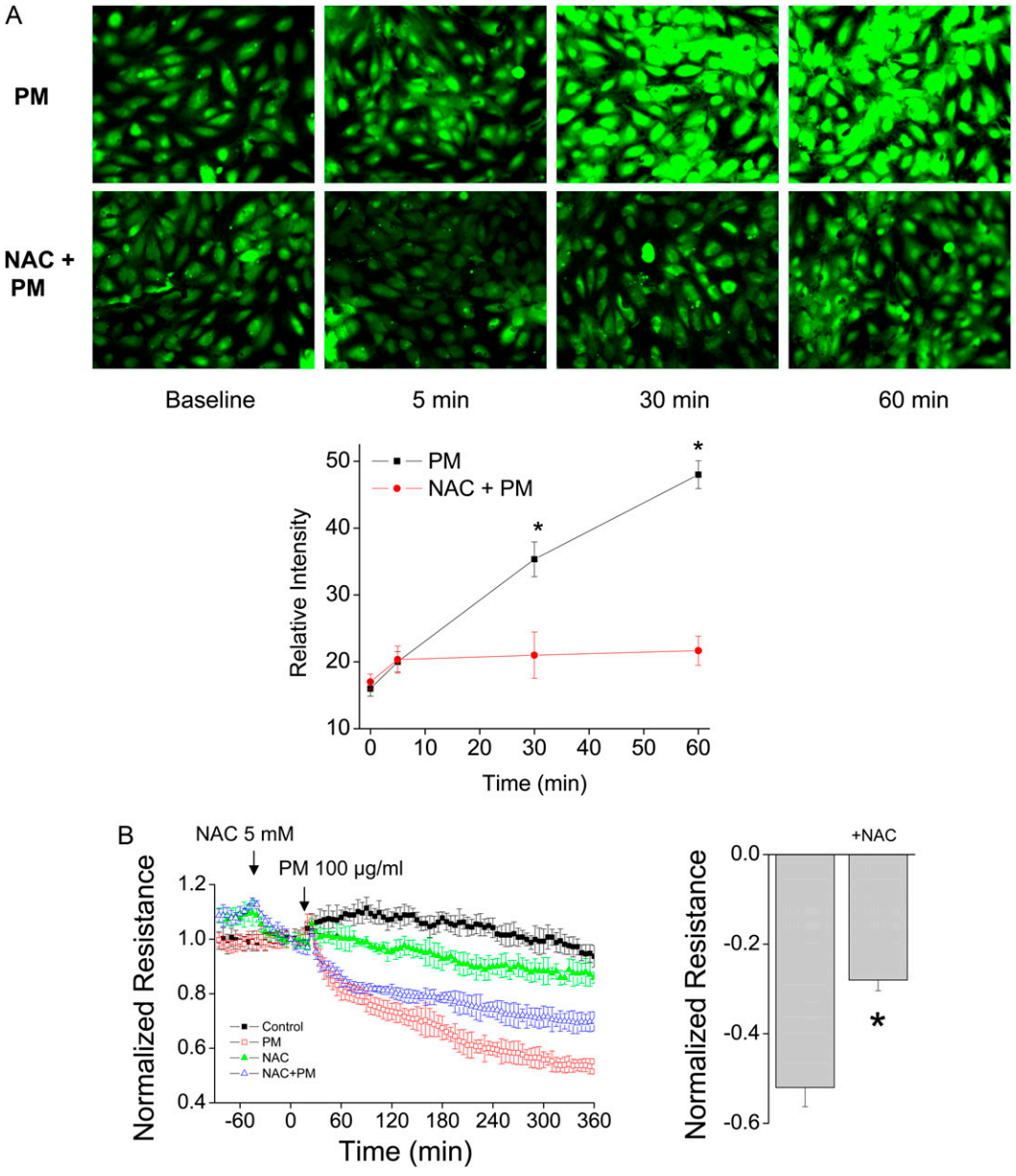

Figure 2. Baltimore tunnel PM increases endothelial reactive oxygen species (ROS) production and mediates EC barrier disruption. (*A*) PM induced EC ROS production (DCFDA fluorescence) in a time-dependent manner. N-acetyl-cysteine (NAC, 5 mM, 1 h pretreatment) prevented PM-induced ROS production in human lung ECs. (*B*) NAC (5 mM, 1 h pre-treatment) inhibits PM-induced EC barrier disruption significantly. Bar graph summarizes PM-reduced normalized resistance (6 h) in three repeated assays (*$P < 0.05$).

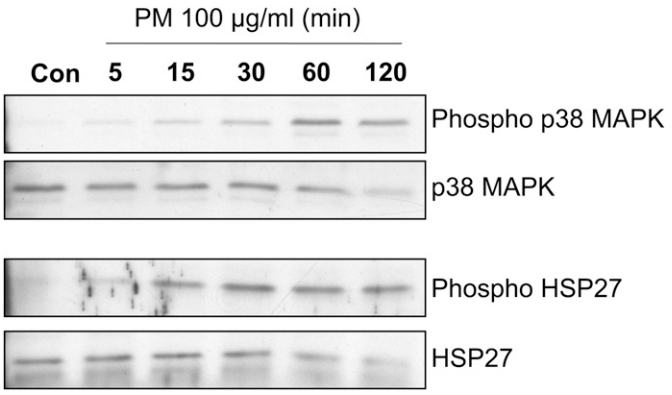

Figure 3. PM Activates p38 mitogen-activated protein kinase (MAPK) and Increases HSP27 Phosphorylation. PM (100 μg/ml) promoted activation of p38 MAPK via phosphorylation in a time-dependent manner (0–1 h), which starts from 5 minutes and peaks at 1 hour. PM also induced phosphorylation of the actin-binding protein HSP27, in a time-dependent manner (0–1 h), which starts from 10 minutes and keeps elevated until 1 hour.

in vitro (8, 23). To directly address whether PM-induced EC barrier function disruption is dependent on stimulation of ROS production, we determined that PM (100 μg/ml) induces substantial EC ROS production as measured by DCFDA oxidation (Figure 2A). EC pretreatment with N-acetyl-cysteine (NAC, 5 mM, 1 h), an ROS scavenger, prevented ROS production induced by PM and significantly inhibited PM-mediated EC barrier disruption (Figure 2B). The PM-insoluble fraction (PM-ISF), the PM component that produced EC barrier disruption, generated increased EC ROS, whereas the soluble PM fraction (PM-SF) failed to do so (Figure E2). These results indicate that PM induces EC barrier disruption, which is partially dependent on ROS generation.

Involvement of p38 MAPK in PM-Induced EC Barrier Disruption

We next examined cell signaling pathways potentially activated via PM-stimulated ROS generation. Initial experiments determined that PM challenge increases p38 MAPK phosphorylation (indicating kinase activation) for up to 60 minutes (Figure 3). We confirmed p38 MAPK activity activation by PM in a time-dependent manner (Cell Signaling) (Figure E3A) and subsequently determined that a prominent p38 MAPK target, the Ser/Thr kinase MAPKAP2, is also activated by PM, as evidenced by phosphorylation of the actin-binding protein, HSP27. These events are again consistent with PM-mediated activation of p38 MAPK (10). Consistent with a role for p38 MAPK in PM-mediated EC barrier dysfunction, pretreatment with the selective p38 MAPK inhibitor, SB 203580 (10 μM), partially attenuated declines in EC TER values induced by PM (~40% inhibition) (Figure 4). Furthermore, reductions in expression of p38 MAPK subtypes (α, β, γ, δ) via siRNA treatment resulted in attenuation of EC barrier disruption induced by PM in an isotype-specific manner (data not shown). For example, reductions in expression of p38 MAPK α or γ subtype failed to alter PM-induced EC barrier disruption, whereas reduced expression of the p38 MAPK β isoform significantly inhibited PM-induced barrier disruption (~50%) (Figure 5). Finally, we observed increased phosphorylation of the stress-induced protein kinase known as JNK by EC exposure to PM treatment. Although JNK was reported to promote HSP27 phosphorylation (24), unlike p38 MAP kinase, selective JNK inhibition by JNKI1 failed to alter PM-induced EC barrier disruption (data not shown). Together, these observations indicate that the p38 MAPK β isoform, but not JNK, is involved in mediating PM-induced EC barrier disruption.

Involvement of HSP27 in PM-Induced Paracellular Gap Formation and Barrier Disruption

We next examined the role of the actin-binding protein, HSP27, in the regulation of PM-induced EC barrier disruption. Like p38 MAPK, reductions in HSP27 expression (siRNA) reduced PM-induced EC barrier disruption (~36%) (Figure 6A), whereas pretreatment with NAC (5 mM) abolished PM-induced p38 MAPK phosphorylation and HSP27 phosphorylation (Figure 6B). Similar results were observed with SB203580 (10 μM), a selective inhibitor of p38 MAPK α and β subtypes, which inhibited p38 MAPK activity (Figure E3B) and dramatically attenuated both PM-induced p38 MAPK phosphorylation and HSP27 phosphorylation (Figure 6B).

Alterations in endothelial barrier functions are intimately linked to alterations in the endothelial actin cytoskeleton (21), and it is well known that the phosphorylation of HSP27 leads to stress fiber and paracellular gap formation in EC (10). We examined actin organization in PM-challenged EC monolayers and noted that under basal conditions, actin was arranged in a fine reticular pattern partially localized at the cell periphery (Figure 7). In contrast, PM challenge (10–100 μg/ml, 1 h) increased F-actin fluorescence, increased actin organization into axially oriented stress fibers, and resulted in formation of paracellular gaps (Figure 7, *solid arrow*). Pretreatment of EC monolayers with either NAC (5 mM) or SB (10 μM) prevented gap formation induced by PM (Figure 7). These data strongly suggest that PM induces EC barrier disruption via cytoskeletal rearrangement into a contractile phenotype, which is dependent on ROS and p38 MAPK activation.

DISCUSSION

Epidemiologic studies have firmly linked increased ambient PM exposure to increased cardiopulmonary morbidity and mortality (1). Despite strong epidemiologic evidence, our understanding of the biological mechanisms for these adverse outcomes remains incomplete. We recently determined that intratracheal delivery of an ambient PM suspension in mice induced acute lung inflammation marked by leukocyte recruitment into the lung and highly significant protein leakage into bronchoalveolar fluid, reflecting breach of endothelial and epithelial cell barriers (9). As our preliminary studies failed to observe obvious PM-mediated disruption of epithelial monolayer barrier integrity reflected by TER (unpublished observations), we hypothesized that active PM components may disrupt lung endothelial barrier integrity, resulting in elevated vascular permeability and protein leakage into lung tissues. In addition to the lung microcirculation, PM gain access to multiple vascular beds including coronary and arterial circulations, with the potential for increasing local oxidative stress and proinflammatory effects.

In the present study, we have demonstrated that PM increases paracellular gap formation with significant loss of EC barrier integrity. This disruption in vascular integrity with resultant increases in permeability is an essential feature of inflammatory processes such as acute lung injury and sepsis, and contributes significantly to the high morbidity and mortality of these conditions. This study provides evidence of the direct disruption of EC barrier by PM *in vitro*, and explains the potential molecular mechanism of PM-induced acute/chronic

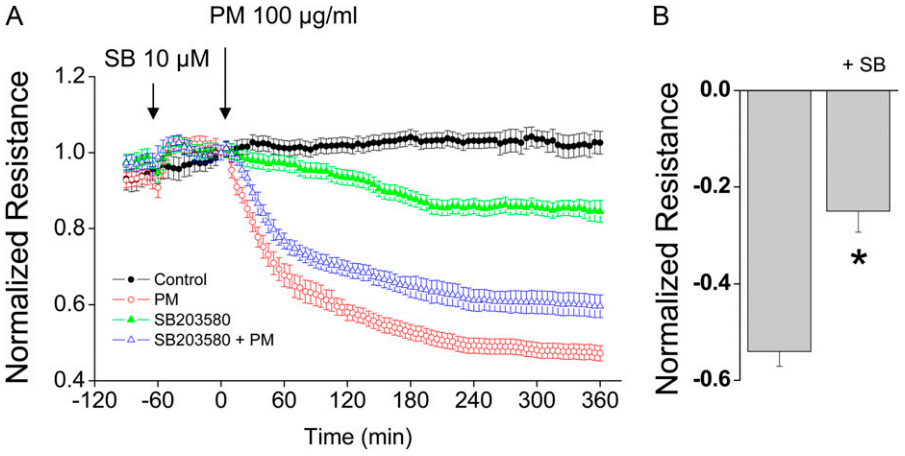

Figure 4. p38 MAPK significantly contributes to PM-induced EC barrier disruption. (*A*) The p38 MAPK inhibitor, SB203580 (10 μM, 1 h pretreatment), prevented PM-induced EC barrier disruption significantly. (*B*) Bar graph summarizes PM-reduced normalized resistance (6 h) in three repeated assays (*$P < 0.05$).

lung damage, which contributes to numerous cardiopulmonary outcomes. The data presented in this report demonstrate that PM rapidly stimulates ROS generation in human lung vascular endothelium, resulting in increased p38 MAPK activation, HSP27 phosphorylation, and a marked disruption in EC monolayer integrity and barrier function via cytoskeletal rearrangement. As endothelial cell barrier integrity is key to lung homeostasis and the prevention of environmental toxins from

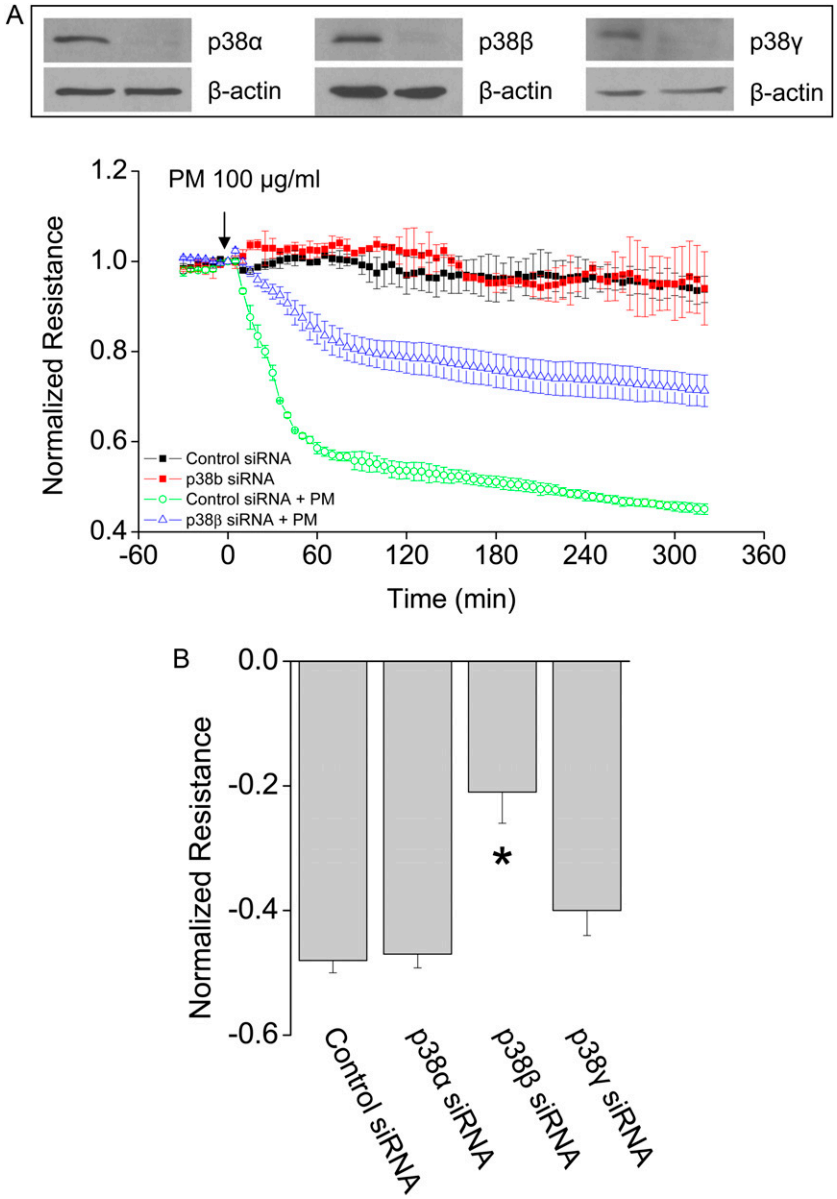

Figure 5. p38 MAPK β but not p38 MAPK α contributes to PM-induced EC barrier disruption. siRNA samples of p38 MAPK α, p38 MAPK β, or p38 MAPK γ (100 ng/ml) greatly reduced their protein levels in EC (> 90%). (*A*) p38 MAPK α or p38 MAPK γ siRNA did not affect PM-induced EC barrier disruption; instead, siRNA of p38 MAPK β partially prevented PM-induced EC barrier disruption. (*B*) Bar graph summarizes corresponding PM-reduced normalized resistance in three repeated assays in ECs with different siRNA treatment (*$P < 0.05$).

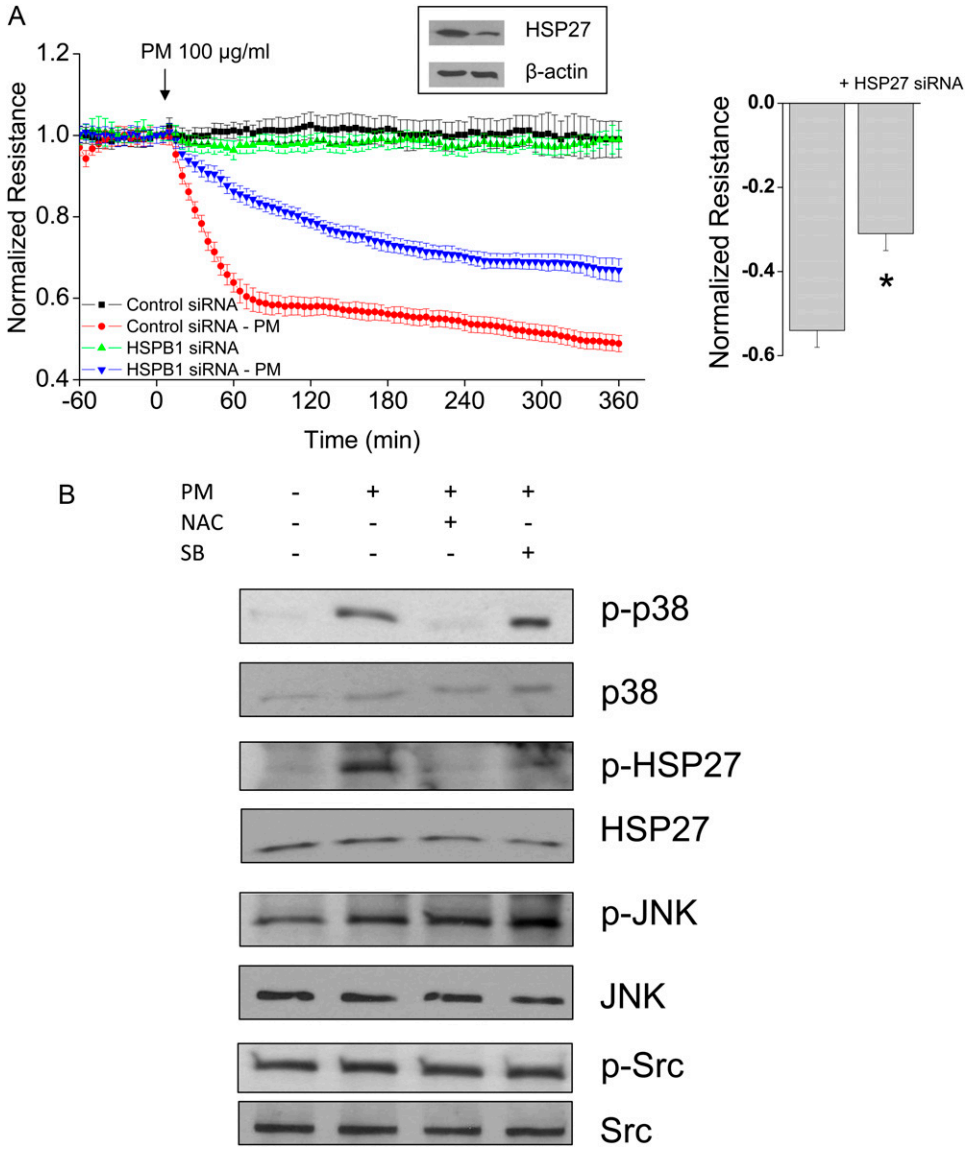

Figure 6. HSP27 contributes to PM-induced EC barrier disruption. (*A*) PM-induced EC barrier disruption is significantly prevented by HSP27 siRNA treatment, which greatly decreased EC HSP27 protein level (> 80%). Bar graph summarizes PM-reduced normalized resistance (6 h) in three repeated assays (*$P < 0.05$). (*B*) PM (100 μg/ml, 1 h) induced HSP27 phosphorylation was dependent on an ROS–p38 MAPK pathway. ROS scavenger NAC (5 mM, 1 h pretreatment) inhibited PM-induced p38 MAPK activation and HSP27 phosphorylation. p38 MAPK inhibitor SB203580 (10 μM, 1 h pretreatment) prevented phosphorylation of HSP27 by PM. Phosphorylation of JNK or Src was not affected by NAC or SB203580 pretreatment.

accessing other physiologic systems, this pathway contributes to acute inflammatory lung injury (25) and potentially contributes to PM-induced cardiopulmonary dysfunction.

ROS and other mechanisms have been proposed to explain the adverse health effects of particulate pollutants including inflammation, autonomic nervous system dysfunction, procoagulant effects, and covalent modification of cellular components (26, 27). Extensive ROS activation by PM induces increased activity of the transcription factor, nuclear factor erythroid 2-related factor 2 (Nrf2), which leads to protective responses via transcrip-

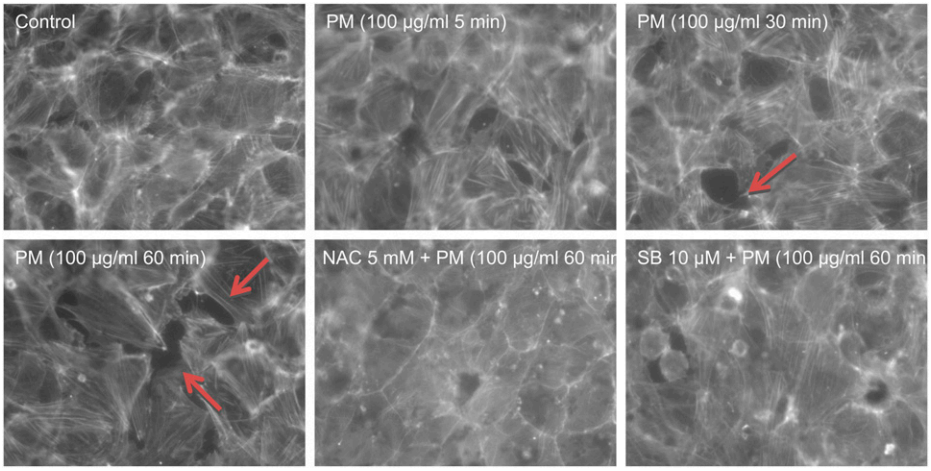

Figure 7. NAC and SB203580 inhibit PM-induced gap formation. PM (100 μg/ml, 1 h) induced increases in stress fiber and formations of paracellular gap (shown by *arrows*) in human lung ECs. NAC (5 mM, 1 h pretreatment) or SB203580 (10 μM, 1 h pretreatment) prevented both the increase of stress fiber and formation of gap induced by PM challenge.

tional activation of over 200 antioxidant and detoxification enzymes, collectively known as the phase 2 response (28). A further increase in ROS production can result in proinflammatory and cytotoxic effects. In the endothelium, it is necessary to point out that other PM chemicals and transition metals play a key role in ROS overproduction. For example, it has been demonstrated that metals associated with PM exert a proinflammatory effect in the respiratory system and the generation of ROS, possibly via transition metals (e.g., Fe, Ni, Cu, Co, and Cr) or polycyclic aromatic hydrocarbon (PAH) (29). These components mainly exist as water-insoluble components of PM, which exert effects similar to those of whole PM. These transitional metal components are potentially inhaled, translocated to endothelium, and induce local increases in ROS production. In this present study, we have focused on the ROS-mediated effects on EC barrier dysfunction evoked by PM. Future studies will be designed to resolve the non–ROS-dependent pathways, such as ROS-independent IL-6 activation (18).

A key finding of our study is that PM-induced endothelial disruption is selectively regulated by p38 MAPK β isoform. p38 MAPK isoforms are members of a larger group of serine/threonine protein kinases, which allow the transduction of extracellular stress signals to the cell nucleus. There are four p38 MAPKs in mammals: α, β, γ, and δ, which are further divided into two distinct subsets (α/β versus γ/δ). This is evident not only from amino acid sequence identity, but also from their susceptibilities to inhibition by SB203580 and SB202190 with p38 MAPK α and p38 MAPK β inhibited by these compounds, whereas p38 MAPK γ and p38 MAPK δ are unaffected (30). In the endothelial cells, p38 MAPK α and p38 MAPK β are the major types with mRNA levels of 41% and 36%, respectively, and 10 μM SB203580 inhibits over 80% of this p38 activity (31). Very few studies have characterized differences in substrate selectivity of p38 MAPK α and p38 MAPK β, and a selective inhibitor of either p38 MAPK α or p38 MAPK β does not currently exist. Our finding that PM selectively activates p38 MAPK β provided a novel approach to potentially define differential biochemical functions of p38 MAPK α and p38 MAPK β. In this regard, prior reports indicate that the chrysene component in PM stimulate MAPK activation (32) with benzopyrene-7,8-diol-9,10-epoxide (BPDE) as well as chrysene-1,2-diol-3,4-epoxide, common components in particulate air pollution, rapidly activate p38 MAPK and JNK (33). Further interrogation of the specific PM component or cellular factor that selectively activates p38 MAPK β may provide novel insights into p38 MAPK β activities in endothelial cells.

In this study, we demonstrated that a solution of PM at concentrations of 10 to 100 μg/ml are sufficient to induce EC barrier disruption, a finding of interest when one considers that the concentration of PM within tunnels may exceed 100 $\mu g/m^3$. A healthy adult working or driving in this environment with an average ventilation of 10 L/minute causes his or her alveolar epithelial cell exposure to a PM concentration as high as 1.5 to 3 μg/ml/hour in the 20 to 40 ml epithelial lining fluid (34). Under these conditions, a single work week of PM exposure (5 d or 40 h) will result in accumulated total exposure of 60 to 120 μg/ml, a concentration which induces significant endothelial permeability changes (35). Future studies will localize PM in lung tissue of different animal models by use of fluorescent labeled PM via intratracheal instillation, allowing the tracking of PM absorption/translocation/elimination, and further address PM-induced EC barrier disruption *in vivo*.

The translocation of PM particles, especially fine components, across the alveolar–blood barrier has been demonstrated in animal studies with PM delivered by inhalation and instillation (35–37). The fine particles are the most likely to account for the induced endothelial oxidative stress generated in this model. Elevations in oxidative stress within lung epithelium exposed to PM (18) produces subsequent increases in IL-6 and increases lung inflammation via increased neutrophil infiltration and lung vasculature permeability (38). As noted earlier, besides human pulmonary artery endothelium (which we have used in these studies), lung microvascular EC is also a primary target of PM. We observed PM to induce similar activation of the pathway involving ROS-p38 MAPK-HSP27 in microvascular EC (Figure E4). More studies should be designed to compare the effects of PM on different EC types in terms of the phenotypic heterogeneity in lung endothelium before these findings could be translated to further *in vivo* studies.

In summary, this study demonstrates the direct capacity for PM to induce ROS and mediate ROS-dependent signaling, which results in paracellular gap formation and endothelial barrier disruption. EC barrier disruption induced by PM is dependent on ROS-activated p38 MAPK β and subsequent phosphorylation of HSP27, which results in cytoskeletal rearrangement and EC barrier disruption. Scavenging of ROS, inhibition or reduced expression of p38 MAPK (especially p38 MAPK β), or reduced expression of HSP27 prevented EC barrier disruption caused by PM. These novel ROS-dependent pathways that regulate p38 MAPK subtype activation, HSP27 phosphorylation, and EC barrier disruption by PM elucidate potential targets to minimize the proinflammatory responses and cardiopulmonary events associated with the inhalation of environmental air pollutants. These results demonstrate that PM induces ROS generation in human lung endothelium, resulting in oxidative stress–mediated EC barrier disruption via p38 MAP kinase– and HSP27-dependent pathways. These findings support a novel mechanism for PM-induced lung dysfunction and potential adverse cardiovascular outcomes.

Conflict of Interest Statement: None of the authors has a financial relationship with a commercial entity that has an interest in the subject of this manuscript.

Acknowledgments: The authors gratefully acknowledge the contribution of Lakshmi Natarajan for expert technical assistance.

References

1. Dominici F, Peng RD, Bell ML, Pham L, McDermott A, Zeger SL, Samet JM. Fine particulate air pollution and hospital admission for cardiovascular and respiratory diseases. *JAMA* 2006;295:1127–1134.
2. Gurgueira SA, Lawrence J, Coull B, Murthy GG, Gonzalez-Flecha B. Rapid increases in the steady-state concentration of reactive oxygen species in the lungs and heart after particulate air pollution inhalation. *Environ Health Perspect* 2002;110:749–755.
3. Nemmar A, Hoylaerts MF, Hoet PH, Dinsdale D, Smith T, Xu H, Vermylen J, Nemery B. Ultrafine particles affect experimental thrombosis in an *in vivo* hamster model. *Am J Respir Crit Care Med* 2002;166:998–1004.
4. Gold DR, Litonjua A, Schwartz J, Lovett E, Larson A, Nearing B, Allen G, Verrier M, Cherry R, Verrier R. Ambient pollution and heart rate variability. *Circulation* 2000;101:1267–1273.
5. Elder A, Oberdorster G. Translocation and effects of ultrafine particles outside of the lung. *Clin Occup Environ Med* 2006;5:785–796.
6. Suwa T, Hogg JC, Quinlan KB, Ohgami A, Vincent R, van Eeden SF. Particulate air pollution induces progression of atherosclerosis. *J Am Coll Cardiol* 2002;39:935–942.
7. Nurkiewicz TR, Porter DW, Barger M, Castranova V, Boegehold MA. Particulate matter exposure impairs systemic microvascular endothelium-dependent dilation. *Environ Health Perspect* 2004;112:1299–1306.
8. Li Z, Hyseni X, Carter JD, Soukup JM, Dailey LA, Huang YC. Pollutant particles enhanced H_2O_2 production from nad(p)h oxidase and mitochondria in human pulmonary artery endothelial cells. *Am J Physiol* 2006;291:C357–C365.
9. Wang T, Moreno-Vinasco L, Huang Y, Lang GD, Linares JD, Goonewardena SN, Grabavoy A, Samet JM, Geyh AS, Breysse PN, *et al.* Murine lung responses to ambient particulate matter: genomic analysis and influence on airway hyperresponsiveness. *Environ Health Perspect* 2008;116:1500–1508.

10. Dudek SM, Garcia JG. Cytoskeletal regulation of pulmonary vascular permeability. *J Appl Physiol* 2001;91:1487–1500.
11. Parsons PE, Worthen GS, Moore EE, Tate RM, Henson PM. The association of circulating endotoxin with the development of the adult respiratory distress syndrome. *Am Rev Respir Dis* 1989;140:294–301.
12. The acute respiratory distress syndrome network. Ventilation with lower tidal volumes as compared with traditional tidal volumes for acute lung injury and the acute respiratory distress syndrome. *N Engl J Med* 2000;342:1301–1308.
13. Williams MA, Porter M, Horton M, Guo J, Roman J, Williams D, Breysse P, Georas SN. Ambient particulate matter directs nonclassic dendritic cell activation and a mixed Th1/Th2-like cytokine response by naive CD4+ t cells. *J Allergy Clin Immunol* 2007;119:488–497.
14. Porter M, Karp M, Killedar S, Bauer SM, Guo J, Williams D, Breysse P, Georas SN, Williams MA. Diesel-enriched particulate matter functionally activates human dendritic cells. *Am J Respir Cell Mol Biol* 2007;37:706–719.
15. Walters DM, Breysse PN, Schofield B, Wills-Karp M. Complement factor 3 mediates particulate matter-induced airway hyperresponsiveness. *Am J Respir Cell Mol Biol* 2002;27:413–418.
16. Walters DM, Breysse PN, Wills-Karp M. Ambient urban baltimore particulate-induced airway hyperresponsiveness and inflammation in mice. *Am J Respir Crit Care Med* 2001;164:1438–1443.
17. Williams MA, Rangasamy T, Bauer SM, Killedar S, Karp M, Kensler TW, Yamamoto M, Breysse P, Biswal S, Georas SN. Disruption of the transcription factor nrf2 promotes pro-oxidative dendritic cells that stimulate Th2-like immunoresponsiveness upon activation by ambient particulate matter. *J Immunol* 2008;181:4545–4559.
18. Zhao Y, Usatyuk PV, Gorshkova IA, He D, Wang T, Moreno-Vinasco L, Geyh AS, Breysse PN, Samet JM, Spannhake EW, *et al.* Regulation of COX-2 expression and IL-6 release by particulate matter in airway epithelial cells. *Am J Respir Cell Mol Biol* 2009;40:19–30.
19. Dudek SM, Camp SM, Chiang ET, Singleton PA, Usatyuk PV, Zhao Y, Natarajan V, Garcia JG. Pulmonary endothelial cell barrier enhancement by fty720 does not require the s1p1 receptor. *Cell Signal* 2007; 19:1754–1764.
20. Verin AD, Liu F, Bogatcheva N, Borbiev T, Hershenson MB, Wang P, Garcia JG. Role of ras-dependent ERK activation in phorbol ester-induced endothelial cell barrier dysfunction. *Am J Physiol Lung Cell Mol Physiol* 2000;279:L360–L370.
21. Dudek SM, Jacobson JR, Chiang ET, Birukov KG, Wang P, Zhan X, Garcia JG. Pulmonary endothelial cell barrier enhancement by sphingosine 1-phosphate: roles for cortactin and myosin light chain kinase. *J Biol Chem* 2004;279:24692–24700.
22. Usatyuk PV, Romer LH, He D, Parinandi NL, Kleinberg ME, Zhan S, Jacobson JR, Dudek SM, Pendyala S, Garcia JG, *et al.* Regulation of hyperoxia-induced nadph oxidase activation in human lung endothelial cells by the actin cytoskeleton and cortactin. *J Biol Chem* 2007;282:23284–23295.
23. Dong F, Zhang X, Wold LE, Ren Q, Zhang Z, Ren J. Endothelin-1 enhances oxidative stress, cell proliferation and reduces apoptosis in human umbilical vein endothelial cells: role of etb receptor, nadph oxidase and caveolin-1. *Br J Pharmacol* 2005;145:323–333.
24. Benjamin IJ, McMillan DR. Stress (heat shock) proteins: molecular chaperones in cardiovascular biology and disease. *Circ Res* 1998;83: 117–132.
25. Medeiros N Jr, Rivero DH, Kasahara DI, Saiki M, Godleski JJ, Koutrakis P, Capelozzi VL, Saldiva PH, Antonangelo L. Acute pulmonary and hematological effects of two types of particle surrogates are influenced by their elemental composition. *Environ Res* 2004;95:62–70.
26. Nel A, Xia T, Madler L, Li N. Toxic potential of materials at the nanolevel. *Science (New York, NY)* 2006;311:622–627.
27. Li N, Xia T, Nel AE. The role of oxidative stress in ambient particulate matter-induced lung diseases and its implications in the toxicity of engineered nanoparticles. *Free Radic Biol Med* 2008;44:1689–1699.
28. Cho HY, Reddy SP, Kleeberger SR. Nrf2 defends the lung from oxidative stress. *Antioxid Redox Signal* 2006;8:76–87.
29. Carter JD, Ghio AJ, Samet JM, Devlin RB. Cytokine production by human airway epithelial cells after exposure to an air pollution particle is metal-dependent. *Toxicol Appl Pharmacol* 1997;146:180–188.
30. Cuenda A, Rousseau S. p38 map-kinases pathway regulation, function and role in human diseases. *Biochim Biophys Acta* 2007;1773:1358–1375.
31. Hale KK, Trollinger D, Rihanek M, Manthey CL. Differential expression and activation of p38 mitogen-activated protein kinase alpha, beta, gamma, and delta in inflammatory cell lineages. *J Immunol* 1999;162:4246–4252.
32. Arif JM, Smith WA, Gupta RC. DNA adduct formation and persistence in rat tissues following exposure to the mammary carcinogen dibenzo[a,l]pyrene. *Carcinogenesis* 1999;20:1147–1150.
33. Li J, Chen H, Ke Q, Feng Z, Tang MS, Liu B, Amin S, Costa M, Huang C. Differential effects of polycyclic aromatic hydrocarbons on transactivation of AP-1 and NF-kappaB in mouse epidermal cl41 cells. *Mol Carcinog* 2004;40:104–115.
34. Rennard SI, Basset G, Lecossier D, O'Donnell KM, Pinkston P, Martin PG, Crystal RG. Estimation of volume of epithelial lining fluid recovered by lavage using urea as marker of dilution. *J Appl Physiol* 1986;60:532–538.
35. Karoly ED, Li Z, Dailey LA, Hyseni X, Huang YC. Up-regulation of tissue factor in human pulmonary artery endothelial cells after ultrafine particle exposure. *Environ Health Perspect* 2007;115:535–540.
36. Kreyling WG, Semmler M, Erbe F, Mayer P, Takenaka S, Schulz H, Oberdorster G, Ziesenis A. Translocation of ultrafine insoluble iridium particles from lung epithelium to extrapulmonary organs is size dependent but very low. *J Toxicol Environ Health* 2002;65: 1513–1530.
37. Oberdorster G, Sharp Z, Atudorei V, Elder A, Gelein R, Lunts A, Kreyling W, Cox C. Extrapulmonary translocation of ultrafine carbon particles following whole-body inhalation exposure of rats. *J Toxicol Environ Health* 2002;65:1531–1543.
38. Tao F, Gonzalez-Flecha B, Kobzik L. Reactive oxygen species in pulmonary inflammation by ambient particulates. *Free Radic Biol Med* 2003;35:327–340.